INTRA-TRAIN LONGITUDINAL FEEDBACK FOR BEAM STABILIZATION AT FLASH

W. Koprek*, C. Behrens, M. K. Bock, M. Felber, P. Gessler, K. Hacker, H. Schlarb, C. Schmidt, B. Steffen, S. Wesch, DESY, Hamburg, Germany
S. Schulz, Hamburg University, Germany
J. Szewinski, The Andrzej Soltan Institute for Nuclear Studies, Swierk, Poland

Abstract

The Free electron LASer at Hamburg (FLASH) is a linear accelerator of 330 m length. It provides laser pulses with pulse duration between 10 and hundreds of fs in the soft X-ray wavelength range below 5 nm produced in SASE process from electron bunches with an energy up to 1.2 GeV. FLASH works in pulsed mode with a repetition rate of 10 Hz where up to 800 bunches at a bunch spacing of 1 μs are accelerated in one macro-pulse. The electron beam time structure is well suited for fast intra-train feedbacks using beam based measurements incorporated to the Low Level Radio Frequency (LLRF) control system. The feedback allows further improving the bunch compressions, bunch arrival and bunch energy stability which directly impact the quality of the FEL photon beam. In this paper, we present the beam based signal pre-processing, the implementation into LLRF system, the mandatory exception handling for robust operation and the imbedding of the real-time ~ 2 μs latency fast intra-train feedback with feedbacks for the removal of slow and repetitive errors. First results of the achieved intra-train bunch arrival and peak current stability will be presented together with observed limitations.

INTRODUCTION

The user experiments performed at FLASH impose demanding requirements for bunch train stability. For example, after the FLASH upgrade, a new experiment, called sFLASH, was installed, where the FEL process is seed at the fundamental wavelength [1]. The seeds light pulses of 20 fs duration are produced by high harmonic generation (HHG) when a laser beam passes a gas jet. The HHG light pulses must overlap with the electron bunches in an undulator to initiate the FEL process. Even though, the duration of the electron bunch can be tuned to 260 fs amplitude stability goals of sFLASH require an arrival time jitter below 30 fs [2].

Another example where a high precision synchronization is required are pump-probe experiments at samples with a very low interaction probability. These experiments require a detector signal integration for all bunches across the entire macro pulse to achieve a good signal-to-noise ratio in the detector. The temporal resolution of these experiments is limited by how precise the arrival times of all individual bunches in the pulse train can be stabilized where synchronizations down to sub-10 fs have been requested.

Figure 1 illustrates the layout of the FLASH after upgrade in 2009/2010 [3]. The acceleration section consists of an RF photo-injector electron source, superconducting RF accelerator modules, and two magnetic bunch compressors. At the 30 m long undulator section the FEL beam is produced. During the shutdown, the RF-Gun was exchanged, an accelerator module was exchanged, and a new high-performance accelerator module was installed which allows achieving 1.2 GeV energy of the electron beam. The higher beam energy leads to shorter FEL light pulses with wavelength of 4.45 nm. A new 3.9 GHz superconductive accelerating module with four cavities installed between ACC1 and bunch compressor 2 is used to linearize the energy chirp in the electron bunch before compression. The operation of the 3rd harmonic module allows for tuning the electron pulse duration from ~20 fs to ~300 fs. Finally, a major installation during this shutdown was sFLASH, with the goal to produce longitudinally coherent FEL pulses with narrower spectrum and synchronized to the seed. sFLASH can be operated in parallel to user experiments using the SASE beam from the main undulator.

This paper presents a complete concept of the longitudinal beam based feedback (BBF) algorithms for FLASH. The concept was based on the experience with BBF gathered in the past where the algorithms were tested in bunch compressor 2. More details are presented in [4].

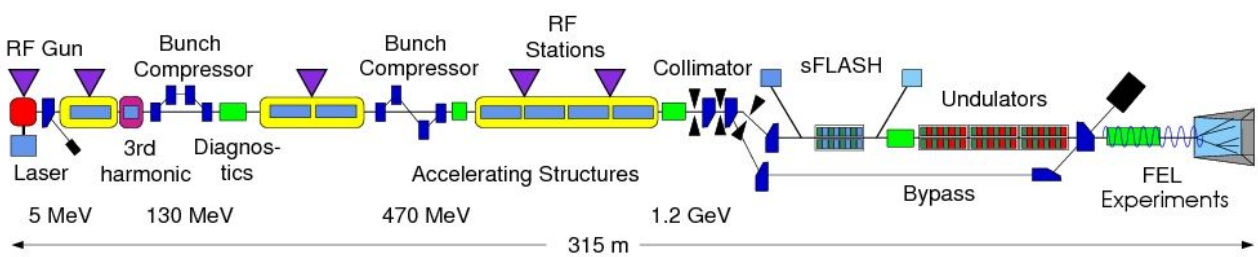

Figure 1: FLASH layout.

* waldemar.koprek@desy.de

CONCEPT OF THE BEAM BASED FEEDBACK

In order to understand the concept of BBF the operation mode of FLASH needs some comment. FLASH operates in pulsed mode with a repetition rate at 10 Hz. Fig. 2 depicts the pulse structure.

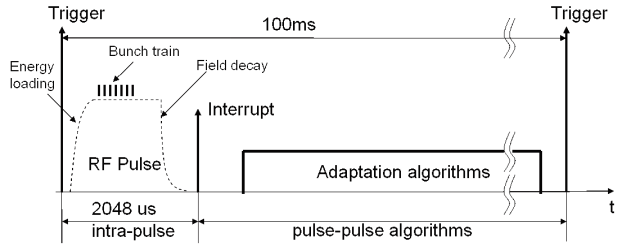

Figure 2: Pulse mode operation scheme.

The RF pulse consists of cavity filling with energy which lasts up to 500 µs followed by a flat energy part where the beam is accelerated. The bunch spacing may vary from 1 µs to 25 µs with maximum bunch train duration of 800 µs. During the bunch train, the fast feedback algorithms modulate the RF drive to the klystron to stabilize the accelerating field. After the RF pulse (approx. ~2 ms) there is 98 ms for pulse-pulse algorithms execution. During this time the front-end CPUs read data from hardware, perform iteration of adaptation algorithms, and send data back to the hardware. The BBF consists of two types of algorithms. One is an intra-bunch train feedback which acts within a few microseconds. Unlike to the intra-pulse LLRF feedback which acts during the entire RF pulse, the intra-train BBF can operate only when data from the beam is available. The second type of BBF uses pulse-to-pulse algorithms running between two subsequent RF pulses in parallel to the LLRF pulse-to-pulse algorithms.

The concept of the longitudinal BBF uses sensors consisting of beam diagnostic devices which measure relevant beam properties and the actuators are the amplitude and phases of the accelerating fields to stabilize the beam properties. The implementation of beam based feedback loops is depicted in Fig. 3. As sensors are used bunch arrival monitors (BAM) and bunch compression monitors (BCM). In addition, the bunch charge is measured using toroids for corrections and exception handling. The first BBF loop is installed in the injector part – the red line. The sensor is one BAM in front of BC2 and the feedback system acts on the RF-gun. The second loop – violet lines – is installed around BC2. The sensors are a BAM and a BCM behind BC2 and a toroid behind accelerating modules. The actuators are two RF systems controlling ACC1 and ACC39 which must correct the field in the modules simultaneously. The third loop is built around BC3 and it is similar to the second one, except there is only one RF system to control the field in modules ACC2 and ACC3. So far, there was tested only the second BBF loop around BC2 and this paper only contains results for that loop.

The LLRF system uses field probes at each cavity to control the acceleration field amplitude and phase of an accelerator module or module-string. This is particularly important during the filling time where no additional information from the electron beam is available. To integrate the BBF, we have chosen controller architecture were the BBF acts on the setpoint of the LLRF system, and the LLRF system regulates in real-time the accelerating field to the new setpoint value. Using this implementation, there are a few advantages like no conflict between LLRF feedback and BBF, full capacity of the LLRF field regulation is used, no need for cross-gain scheduling. It is also easy to implement exception handling.

BEAM DIAGNOSTICS

Bunch Arrival Time Monitor

The goal of the bunch arrival time monitor is to measure the relative arrival time of single bunches with respect to the laser pulses from the optical synchronization system [5]. The fluctuation variation of the bunch arrival time can be used for BBF to correct the amplitude and phase of the accelerating field. Figure 4 depicts a very general diagram of the hardware and firmware of the bunch arrival time monitor. The electron bunch passing pickups installed in the horizontal and the vertical plane of the beam pipe induces short broadband electrical pulses. These pulses are used to modulate the optical pulses emitted from the master laser oscillator in an electro-optical modulator (EOM). Then the modulated and the non-modulated pulses are converted to electrical signals by a photodiode.

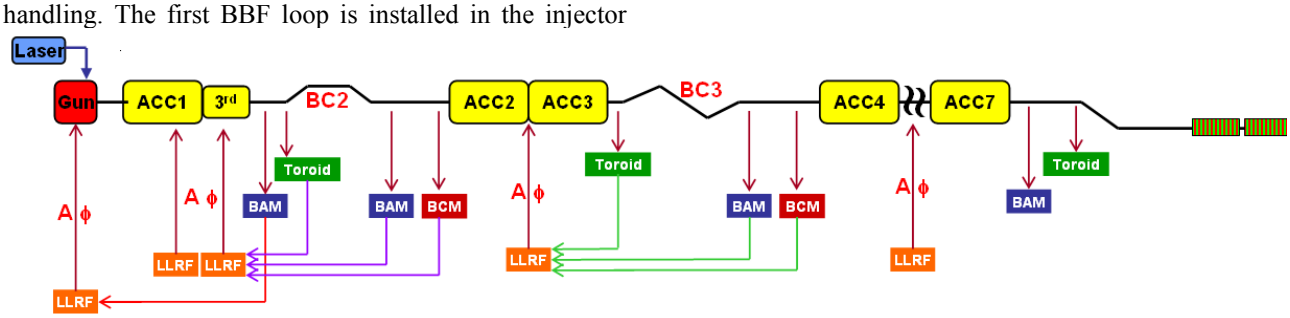

Figure 3: Concept of the beam based feedback.

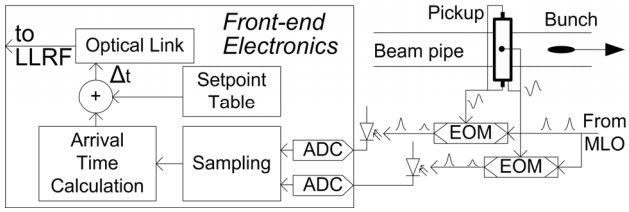

Figure 4: Overview of the bunch arrival monitor.

Next, the electrical signals are digitized in the front-end electronic board called Advanced Carrier Board (ACB). After adjusting the clock delay the peak and baseline of the electric signal are sampled. From the ratio of the modulated to the non-modulated laser pulse amplitudes, the arrival time is retrieved. The computed arrival time is compared with the setpoint SP Table value in SP Table which allows the calculation of the arrival time deviation which in turn is sent digitally through optical gigalink to the LLRF system as an input error signal to the beam feedback [6].

Beam Compression Measurement

The determination of the bunch compression relies on an intensity measurement of emitted coherent diffraction radiation (CDR). Passing a slitted metallic screen, the electron bunches radiate coherently for wavelengths longer than their bunch length. The shorter the bunches, the more the cut-off wavelength of coherent emission reduces, the more intense the total radiation. In Fig. 5 a schematic layout of the BCM setups after the first and second bunch compressor (BC) is shown [7].

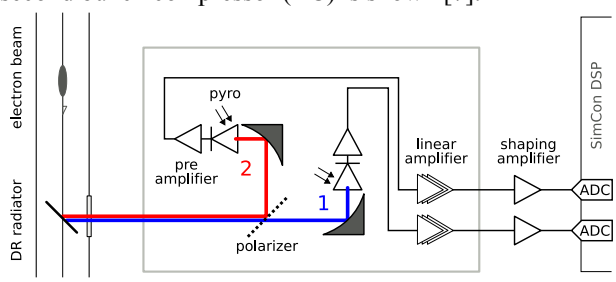

Figure 5: Schematic of bunch compression monitor.

A 45 deg tilt of the diffraction radiator allows guiding the CDR throughout crystalline quartz window into the BCM setup. It is split by a polarizer and focused onto two separated $LiTaO_3$ pyro electric detectors. Using current sensitive preamplifiers with different gain, the dynamic range can be increased. The generated signal with a time constant of 1.4 µs is transformed by a Gaussian shaping amplifier. The chosen pulse width of sigma RMS 250 ns enables a distinction of the compression of each electron bunch in the bunch train. The analog signal is digitized by the 81 MHz ADC of the LLRF SIMCON-DSP board.

Optical Synchronization System

The optical synchronization system is comprised of a master laser oscillator (MLO) narrowband locked to the RF master oscillator of FLASH, a free space distribution system, length stabilized fibre links and different end-nodes for synchronization of experiment lasers, diagnostic components, and optical cross correlators for the injector laser. Newly tested is a commercial SESAM-based laser system Origami-15 which was installed in the synchronization hutch during FLASH upgrade [8]. The measured timing jitter of the optical pulses is 5.2 fs over an offset bandwidth from 1 kHz to 10 MHz. The pulses from the laser are split in the free space distribution unit, amplified in a dispersion compensated Erbium doped fibre amplifier and then sent through the length stabilized optical links to the individual devices of the FLASH facility. Among others the BAMs are the receivers of the 216.66 MHz optical pulses which are then modulated in EOMs to retrieve the bunch arrival times.

Charge Measurement

The charge of individual bunches is measured by toroids installed behind the accelerating modules. Bunches passing the toroid induce electrical pulses with an amplitude proportional to the bunch charge. The sharp pulses are shaped in the front-end electronics and then sent to 81MHz ADCs of the LLRF systems.

LLRF CONTROL SYSTEM

Fig. 6 presents a block diagram of the LLRF system. It consists of an RF master oscillator which generates the low noise 1.3 GHz RF signal to drive the klystron, for the LO generation, and provides the clock signals for operating the digital controller boards.

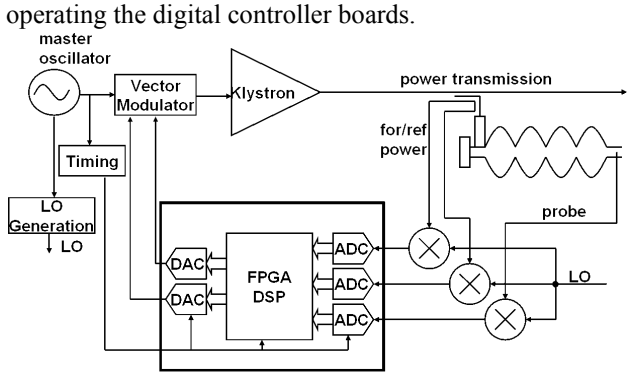

Figure 6: Block diagram of the LLRF system.

During the FLASH shutdown the LLRF systems were substantially upgraded. The old DSP based systems were replaced by new VME cards called SIMCON-DSP. The cards are equipped with 10 ADCs, 4 DACs, a large computation capacity FPGA chip, VME interface, and optical gigalinks for high speed digital communication. These cards were installed for all accelerating modules including RF-gun and the new 3rd harmonic cavity string. The unified hardware for the LLRF systems enabled unification of firmware running in the FPGA chips and to reduce the complexity of the control software. The LLRF software features are: multiple-input-multiple-output (MIMO) controller, toroid based charge measurement,

beam loading compensation, learning feed forward, gain scheduling, feed forward table optimization, output rotation matrix control, and many others. Most of these features were tested in the past [9] and by now they are integrated in one controller. In addition, the control system automatically brings the modules into operation and shut them down by using a finite state machine running in background. Figure 7 depicts a block diagram of the firmware.

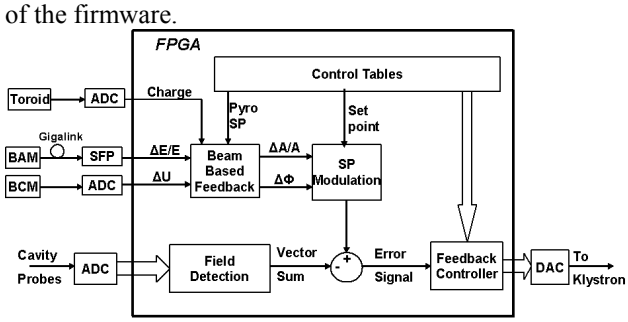

Figure 7: Block diagram of the LLRF firmware.

Eight cavity probes from one cryo-module are connected to the ADCs. The field detection block calculates the field in individual cavities in form of in-phase and quadrature components. Then the signal from each cavity is scaled and rotated to calculate the vector sum which represents the total voltage seen by the beam passing the module. The measured vector sum is compared with the setpoint curve. The error signal is the input to the control part. The feedback controller is implemented as a MIMO controller which generates the control signal sent through DAC outputs to an analog vector modulator connected to the preamplifier driving the klystron [10].

Additional signals from beam diagnostics are connected to the SIMCON-DSP inputs. The analog signal from the toroid is connected to the ADC. Its voltage is proportional to the beam charge passing the module. This signal is measured in real-time with an latency below 1 μs. The second beam signal from the BCM detector is connected to another ADC, and the third one is a digital signal received through the optical link from the ACB board. All three signals are connected to the beam based feedback component which generates two output signals – amplitude and phase modulation of the controller setpoint table. The setpoint table is modulated in real-time and is passed to the feedback algorithms as a new setpoint to which the controller regulates the field in the cavities.

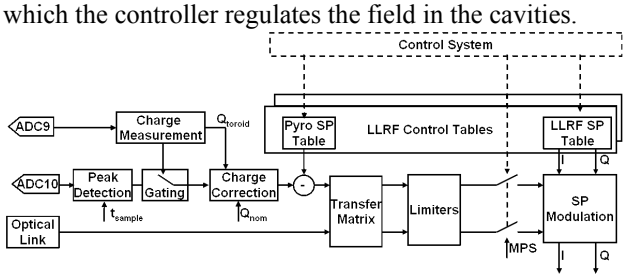

Figure 8: Firmware components of the BBF in the LLRF controller.

Details of the beam based feedback implementation are presented in Fig. 8. The analog signal from the BCM is sampled by an ADC with sampling frequency 81 MHz. The peak detection component decimates the 81 MHz signal to 1 MHz where one sample corresponds to a peak value of the pyro signal for individual bunches. The peak detection component works continuously during the RF pulse and also generates noisy samples when there is no beam.

In order to avoid feeding meaningless noisy samples into the feedback controller the gating components passes through samples only when a beam passes the module. For that purpose, the toroid signal is used and it enables a gate when a beam charge is measured above a user defined threshold. Unfortunately, the pyro signal peak amplitude U_{P_ADC} depends quadratically on the bunch charge Q_T. To eliminate compression measurement errors due to residual small charge fluctuations, first a nominal charge Q_N is defined which corresponds to the average charge value at which the machine is currently operated. The charge corrected compression signal voltage is given by Eq. 1.

$$U_P = \left(\frac{Q_N}{Q_T}\right)^2 U_{P\_ADC} \qquad (1)$$

Since implementation of the formula introduces large latency due to division by Q_T, the above formula was approximated by Eq. 2 for small charge variation around Q_N. For typical charge deviations in the injector of 2% the approximation is off by 0.1% only, which is sufficient for our purpose.

$$U_P = (3 - 2\frac{Q_T}{Q_N})U_{P\_ADC} \qquad (2)$$

The charge corrected pyro signal gives arbitrary information of the bunch compression and the accelerating field should be corrected only when the compression deviates from a given setpoint value. The pyro setpoint theoretically should be a constant value. Unfortunately, due to the hardware design the pyro detector has two drawbacks. It oscillates affecting subsequent bunches and has a pile-up effect which modulates subsequent bunches with a slope. Therefore a pyro setpoint table was implemented in the FPGA in order to cope with these effects. The content of the pyro setpoint table is calculated offline in the control software and it is uploaded to FPGA before beam operation. Both unwanted effects are stationary and the pyro setpoint table is re-loaded only when the operating point is changed. After subtracting the pyro setpoint table from the pyro signal, the pyro error signal together with the BAM error signal, is further processed to determine the required amplitude and phase corrections. The BAM signal received from the ACB card through the optical link is proportional to a relative energy change of the electron bunch through the path length dependent magnetic chicane.

Since the arrival time and the bunch compression are effected by both the amplitude and the phase of the acceleration field the measured errors have to be applied simultaneously on the amplitude and phase of the controller setpoint table. We use a linear approximation for the transfer characteristic which can be described by a 2-by-2 matrix where the outputs are an absolute phase correction and a relative amplitude correction of the setpoint table.

For safety reasons, a limiter module limits the BBF correction signals to ~1% in amplitude and ±1 deg in phase. Both limiters are run-time parameters and can be changed from pulse-to-pulse. The BBF is enabled on request from the control software and it is disabled in real-time by a signal from the machine protection system (MPS) connected to the digital input of SIMCON-DSP. BBF results in amplitude and phase correction signals, but the setpoint table is in form of the I and Q signals. In order to cope with amplitude and phase conversion to I and Q, the setpoint modulation component was implemented according to the equation below.

$$\begin{bmatrix} SP_{I\_O} \\ SP_{Q\_O} \end{bmatrix} = (1+\frac{\Delta A}{A}) \begin{bmatrix} \cos(\varphi) & -\sin(\varphi) \\ \sin(\varphi) & \cos(\varphi) \end{bmatrix} \times \begin{bmatrix} SP_{I\_I} \\ SP_{Q\_I} \end{bmatrix}$$

For small phase errors (|φ| < 1deg), the cos(φ) is approximated by 1 and sin(φ) is approximated by φ. These approximations allow avoiding calculation of sinus and cosine function in the FPGA.

BBF in Bunch Compressor 2

The most challenging issue was the commissioning of the BBF in BC2. As one can see in Fig. 3, there are two accelerating modules running at 1.3 GHz and 3.9 GHz followed by the bunch compressor. The beam properties after BC2 are monitored by a BAM and a BCM. The configuration is depicted in Fig. 9.

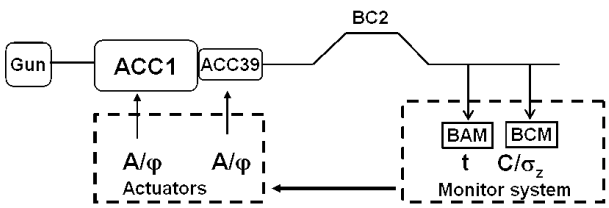

Figure 9: Beam based feedback setup at BC2.

The BBF loop contains two measured values – bunch arrival time Δt_{BC2} and bunch compression ΔC_{BC2} – and four actuators – amplitude and phase in ACC1, $\Delta A_1/A_1$, $\Delta\varphi_1$ and ACC39, $\Delta A_{39}/A_{39}$, $\Delta\varphi_{39}$. In order to project measured values into the actuators corrections we use the following transfer matrix representation as shown in Eq. 3. The first four elements T_{11}, T_{12}, T_{21}, T_{22} are related to amplitude and phase sensivity of module ACC1 and the second four - T_{13}, T_{14}, T_{23}, T_{24} – to ACC39 respectively. The coefficients are used in the Transfer Matrix component as depicted in Fig. 8.

$$\begin{bmatrix} \Delta t_{BC2} \\ \Delta C_{BC2} \end{bmatrix} = \begin{bmatrix} T_{11} & T_{12} & T_{13} & T_{14} \\ T_{21} & T_{22} & T_{23} & T_{24} \end{bmatrix} \begin{bmatrix} \frac{\Delta A_1}{A_1} \\ \Delta\varphi_1 \\ \frac{\Delta A_{39}}{A_{39}} \\ \Delta\varphi_{39} \end{bmatrix} \quad (3)$$

The T-matrix coefficients were found experimentally by scanning the individual amplitude and phase parameters by a small amount around the set values, while the influence on the beam properties was recorded. The relation between LLRF parameter change and beam parameter change was used to determine the T-matrix coefficients. For many accelerator operation settings the ACC1 matrix elements dominate, such that correction of ACC39 can be neglected and the 2x2 matrix is directly inverted. For some machine settings, however, this is not the case. Then the inversion of the T-matrix is performed in least square sense including weighting factors. The least square method ensures that the actuator with the strongest influence is used for correction. With the weighting factors the probability for the actuator to be the jitter source is taken into account. The inverted matrix is then uploaded to the LLRF controller registers before the feedback is closed. After the BBF loop was closed measurements of the beam stability were performed as presented in the next section.

MEASUREMENTS

The main contribution of intra-pulse bunch arrival time deviations is caused by residual beam loading effects on the accelerating field. These control errors are introduced by imperfect feed forward signals, which can not be fully compensated by the feedback controller due to the limited gain. Since this is mainly a repetitive error, it can be reduced by applying iterative learning algorithms that improve the feed forward signal within consecutive pulses. In Fig. 10 a comparison in bunch arrival time between regular and optimized feed forward tables is shown.

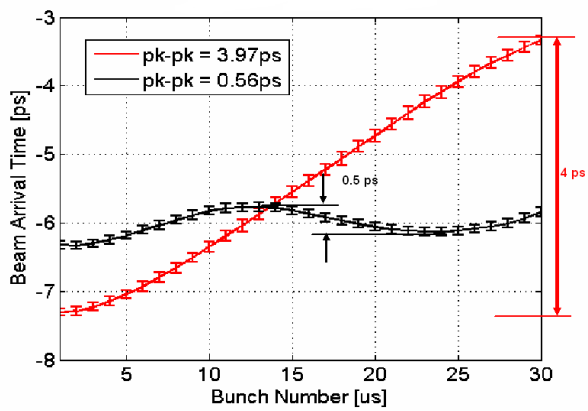

Figure 10: Learning feed forward.

The red one shows a large slope of the arrival time of 30 bunches at the level of 4 ps peak-to-peak which is directly related to the accelerating field slope. Enabling the learning feed forward algorithm flattens the accelerating field and reduces the bunch arrival time deviation to a level of 0.5 ps. The algorithm requires about 50 pulses (5 seconds) to adapt the accelerating field from the red curve to the black curve. The adaptation speed can be regulated by the adaptation gain. However, one has to find a trade-off between the speed of the adaptation and the stability of the algorithm, because fast adaptation may lead to instabilities.

The second part of the test was focused on applying intra-train BBF in BC2. After scanning the transfer matrix the correction coefficients for the ACC1 and the ACC39 LLRF controller were applied. During studies a sequence of 3000 pulses was recorded for different configurations of the machine. During these test we measured the bunch arrival time jitter for individual bunches in the bunch train and the bunch arrival time jitter of the entire bunch trains measured from pulse-to-pulse.

Improvement of the rms arrival time jitter with BBF applied on BC2 is presented in Fig. 11.

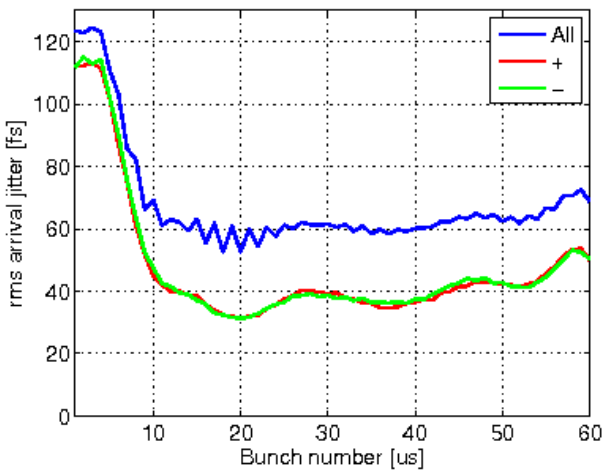

Figure 11: Intra bunch train rms jitter.

The figure shows how the rms arrival time jitter of the bunch changes within a bunch train. One can see from the plot that the latency of the BBF is 4 μs. It means that the BBF after measurements of the first bunch acts on bunch number 5. However the minimal value of the rms jitter is achieved after ~12 bunches due to the time constant of the superconductive cavities. The measured jitter – blue plot in Fig. 11 – was bigger than expected. After careful studies of the machine state it was found that the bunch train coming out from the RF-Gun has enormous oscillations. Further investigations revealed instabilities in the injector laser. The oscillations have a constant frequency of 500 kHz but they change phase, shown in Fig. 12. The plot presents two single shots with a different phase of oscillations. The phase of the oscillation is randomly changing from shot-to-shot and we found the same number of shots with positive and negative versions of the oscillations. Unfortunately due to the high frequency of the oscillation, the BBF cannot remove it. Therefore they are visible even with BBF on. However these oscillations can be easily removed by proper adjustment of the injector laser. If one calculates the rms arrival time jitter from Fig. 11 for 1500 pulses with positive phase of oscillations and then for another 1500 pulses with negative phase, then the shape will look like the green and the red curve.

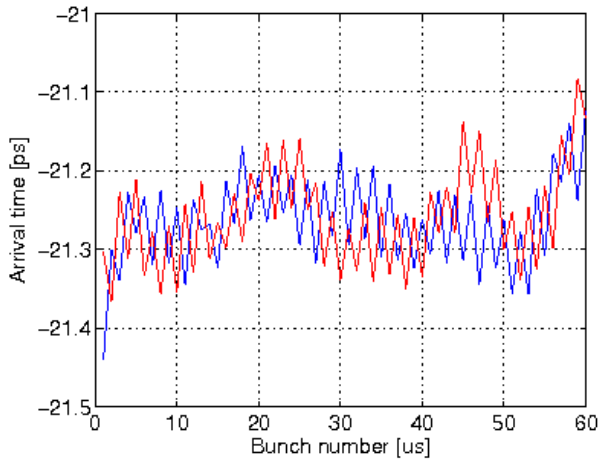

Figure 12: Repetitive oscillations on beam caused by injector laser instability. Two single shots with shifted patterns.

The rms arrival time jitter reduces by ~20 fs and the mean value of the rms jitter is around 40 fs starting from bunch 10 on. This level of beam jitter might be good enough for sFLASH experiments as long as the experiment will use bunch 12 or higher.

The same data was used to calculate the stablility of the bunch train arrival time from pulse-to-pulse. Two measurements were taken to compare the stability with and w/o BBF. The stability was improved from ~70 fs rms without BBF to only 5.0 fs rms when the BBF was applied. Fig. 13 demonstrates the variation of the pulse-train arrival time for a period of 5 minutes.

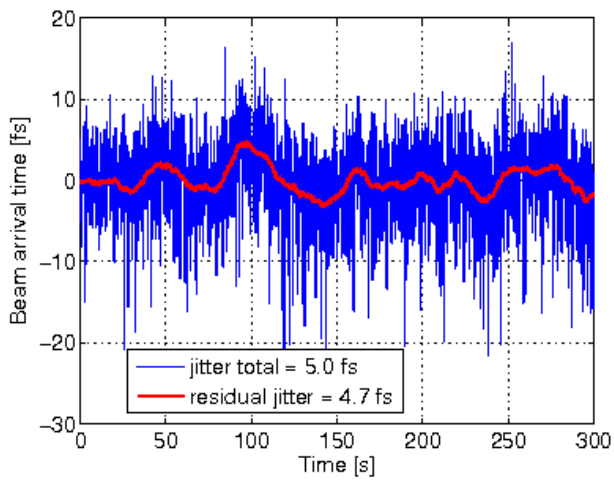

Figure 13: Pulse-pulse stability of the beam - rms jitter of the beam arrival time of the entire bunch train.

CONCLUSIONS AND PLANS

During the short tests of the BBF at FLASH we managed to prove of the concept, where the BBF uses the LLRF systems as actuators and modulates the LLRF set point table without direct interference with the LLRF feedback. The concept is robust also due to implementation of the limiters which prevents the BBF from acting on the LLRF set point in a range bigger than 1% for amplitude and $\pm 1^0$ for phase. The implemented transfer matrix reflects the complex dependencies of amplitude and phase regulation on the beam properties.

The tests showed that the BBF reduced the intra-train bunch arrival time jitter from more than 100 fs to about 40 fs for BC2. The beam arrival time jitter from pulse-to-pulse was reduced from 70 fs to about 5 fs. In addition we demonstrated that the repetitive errors were reduced by learning feed forward algorithm from 4 ps to 0.5 ps.

These positive results stimulate us to also apply the BBF on the RF-gun and for ACC23. Minor automation procedure in order to improve the robustness of the system and to improve the operability for non-experts for every day operation still needs to be added.

Further improvements in speed, quality and robustness could be gained by having BBF signals available in a central place to manage fast feedbacks actions on all LLRF stations simultaneously which would deduce the cross-talk among individual feedbacks.

REFERENCES

[1] J. Boedewadt et al, “sFLASH – First results of a direct seeding at FLASH”, FEL2010, Malmö, August 2010, WEOAI2, http://www.JACoW.org

[2] V. Miltchev et al, “Tolerance Studies on the High-Harmonic Laser Seeding at Flash”, FEL2008, Gyeongju, August 2008, TUPPH003, http://www.JACoW.org

[3] S. Schreiber, “FLASH upgrade and first results”, FEL2010, Malmö, August 2010, TUOBI2, http://www.JACoW.org

[4] F. Loehl et al, “Observation of 40 fs Synchronization of Electron Bunches for FELs”, FEL2008, Gyeongju, August 2008, THBAU02, http://www.JACoW.org

[5] K. Hacker et al, “Beam arrival-time and position measurements using electro-optical sampling of pickup signals”, BIW10, Santa Fe, May 2010, MOFNB02, http://www.JACoW.org.

[6] P. Gessler et al, “Longitudinal Bunch Arrival-Time Feedback at FLASH”, FEL2010, Malmö, August 2010, THPA04, http://www.JACoW.org

[7] C. Behrens et al, “Upgrade and evaluation of the bunch compression monitor at the Free-Electron Laser in Hamburg (FLASH)”, IPAC’10, Kyoto, May 2010, MOPD090, http://www.JACoW.org.

[8] S. Schulz et al, “Performance of the FLASH Optical Synchronization System Utilizing a Commercial SESAM-Based Erbium Laser”, FEL2010, Malmö, August 2010, THPA05, http://www.JACoW.org

[9] S. Simrock et al, “FPGA based digital RF control for FLASH”, LINAC2006, Knoxville, May 2006, THP097, http://www.JACoW.org

[10] W. Jalmuzna, “Multipurpose LLRF field controller for various superconducting cavity applications”, ICALEPCS2009, Kobe, October 2009, TUP069, http://www.JACoW.org